RECENT RESULTS FROM ICECUBE ON NEUTRINO OSCILLATIONS

J. P. A. M. de André, for the IceCube Collaboration[a]
Department of Physics and Astronomy, Michigan State University, East Lansing, MI, USA

The IceCube Neutrino Observatory, located at the South Pole, is the world's largest neutrino detector. IceCube is well placed to probe the existence of sterile neutrinos with $\Delta m^2_{41} \approx 1$ eV^2, which is a region of particular interest for the various anomalies motivating the existence of sterile neutrinos, by looking for muon neutrino disappearance around 1 TeV. In addition to that, using data from a more densely instrumented region of the detector, DeepCore, IceCube can be used to precisely measure regular neutrino oscillations and, by looking at distortions on those oscillations, further probe the existence of sterile neutrinos. We will discuss recent results from IceCube on neutrino oscillations, both related to searches for sterile neutrino and to precision measurement of the atmospheric mixing angles.

1 Introduction

Neutrino oscillations were discovered by Super-Kamiokande in 1998 [1] through the measurement of atmospheric neutrinos, and SNO in 2002 [2] through the measurement of solar neutrinos. The parameters describing the standard three flavor neutrino oscillation have been measured with varying precision by many different experiments (see Ref. [3] and references therein) with the exception of the CP-violating phase (δ_{CP}) and the mass ordering (the sign of Δm^2_{32}). The amplitude of the neutrino oscillation is determined by the elements of the mixing matrix, described by the mixing angles (θ_{12}, θ_{13}, and θ_{23}) and δ_{CP}, while its oscillation period in vacuum depends on $|\Delta m^2_{32}|L/E$ and $|\Delta m^2_{21}|L/E$, where E is the neutrino energy, L is the distance between its production and interaction points, and Δm^2_{ji} is the difference between the square of the masses of ν_j and ν_i.

At about the same time as neutrino oscillations were discovered, evidence for neutrino oscillations was also obtained by LSND [4] corresponding to a different oscillation period than those mentioned above. In order to introduce an additional oscillation period a fourth family of neutrino is needed, however it was experimentally determined that only three light neutrinos couple to the Z^0 boson [5], and therefore additional neutrino families would have to be "sterile", that is not interacting through the Standard Model. The evidence for neutrino oscillations by LSND was however not supported by KARMEN [6], which is very similar to LSND, even if for some regions of the parameter space the LSND oscillation would not have been observed by KARMEN. The case for the existence of sterile neutrinos is further complicated by numerous experimental results favoring and disfavoring their existence (see Ref. [7] and references therein).

We will discuss in this proceeding recent results from IceCube on standard neutrino oscillations and on searches for sterile neutrinos.

2 The IceCube detector

The IceCube Neutrino Observatory [8] is the world's largest neutrino detector, instrumenting about 1 Gton of ice in the deep glacier near the South Pole Station, Antarctica. A total of 5160

[a] see http://icecube.wisc.edu/collaboration/authors/current for full author list

digital optical modules (DOMs) are used to instrument the full volume, as shown in Fig. 1. The observatory was originally designed to detect TeV – PeV neutrinos. An astrophysical component was discovered in this energy range in 2014 [9]. In 2008 the original design was augmented by creating a region, called DeepCore [10], in the deepest, clearest ice and centered in the detector with a higher density of DOMs. This increased density of optical modules over 10 Mton of ice reduces the energy threshold of IceCube from hundreds to a few GeV in this region and makes it possible to perform competitive neutrino oscillation measurements and dark matter searches.

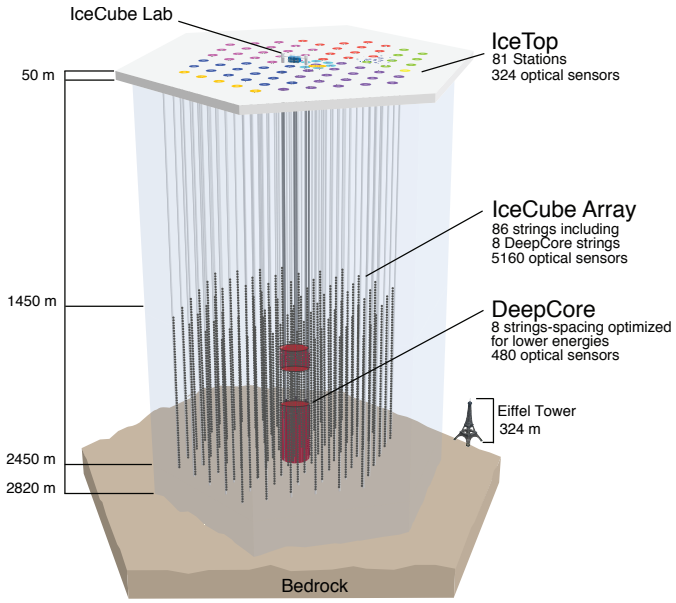

Figure 1 – Diagram of the IceCube Neutrino Observatory at its completion, December 2010, with the denser DeepCore array indicated.

IceCube detects neutrinos by measuring the Cherenkov light produced from charged particles created via the neutrinos interacting in the ice or bedrock. Hadronic or electromagnetic showers produced in the neutrino interaction will emit most of the light close to the vertex, and the observed event is more spherical, as shown in the left panel of Fig. 2. When a muon is produced in the neutrino interaction it propagates through the ice emitting Cherenkov light over a long distance, and the observed event is more elongated, as shown in the right panel of Fig. 2. These two topologies are identified as "cascade-like" and "track-like", respectively.

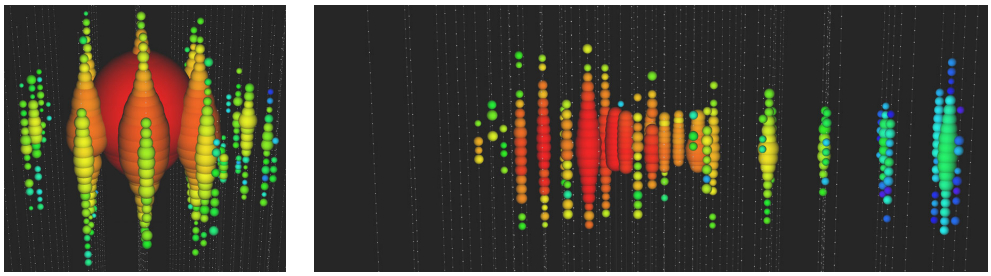

Figure 2 – Example of "cascade-like" (left) and "track-like" (right) events from data [9]. Each sphere corresponds to a DOM having observed some charge, with the size of the sphere depending on the hit charge and the color depending on the hit time.

2.1 Signatures for neutrino oscillations in IceCube

Atmospheric neutrinos are particularly interesting for studying neutrino oscillations because they are produced with energies spanning many orders of magnitude and are available at varying

values of L (from about 20 km to about 12700 km). The energy E is reconstructed based on the light observed in the detector, and neutrino propagation distance L is obtained via the reconstructed neutrino direction.

In the framework of Standard Neutrino Oscillations, the first ν_μ disappearance maximum probability happens around 25 GeV for neutrinos directly up-going, with additional maxima and minima at lower energies. This first disappearance maximum can be observed in the DeepCore array with good precision. In this case the ν_μ oscillate to ν_τ, which will rarely interact in the detector due to the significantly smaller ν_τ cross-section, and because of that we expect the effect of the ν_μ disappearance will show up as a reduction of the neutrino rate in a region of the parameter space corresponding to $L/E \sim 500$ km/GeV.

In addition to that, IceCube can also search for sterile neutrinos by looking for ν_μ disappearance at higher energies, before the regular ν_μ oscillations would take place. Given the favored $\Delta m^2_{41} \sim 1$ eV^2 region for sterile neutrinos [7], we would expect $\nu_\mu \to \nu_s$ to happen at a few TeV for up-going ν_μ. The expected $\nu_\mu \to \nu_s$ oscillation is in fact intensified due to matter effects [11,12,13,14] governed by the Earth's dimensions and matter density profile [15], so that even for small values of the θ_{24} mixing parameter the visible oscillations become enhanced, causing almost complete ν_μ disappearance. In IceCube we can directly look for the $\nu_\mu \to \nu_s$ signature around 1 TeV (high energy signature) in order to observe this resonant-like transition, or we can use DeepCore to evaluate the effect it would have in the standard ν_μ disappearance maximum (low energy signature).

These two approaches for searching sterile neutrinos are very complementary given that the effects that can be studied with each approach are not the same. By looking directly for the high energy signature for sterile neutrinos we can precisely measure the θ_{24} mixing angle and Δm^2_{41}. On the other hand, by looking for the low energy signature for sterile neutrinos we can probe not only the θ_{24} mixing angle but also the θ_{34} mixing angle, however in that case there is only weak dependence on Δm^2_{41}.

3 Search for sterile neutrinos at high energy

The results in this section are published in Ref. [16].

In order to search for sterile neutrino oscillations around 1 TeV, we start from a one year sample of up-going track-like events, composed almost exclusively by ν_μ CC events, that had been used in previous analysis [17]. In this sample the peak of the energy distribution of events is around 1 TeV, which is optimal for a $\Delta m^2_{41} \approx 1$ eV^2 search.

The search for sterile neutrinos is performed by fitting possible sterile neutrino signatures to the observed $E \times \cos\theta_z$ distribution, accounting for possible systematic errors coming from the uncertainties on the neutrino flux and detector. No significant deviation from the null hypothesis was observed, and therefore we can constrain the $\theta_{24} \times \Delta m^2_{41}$ phase space as shown in Fig. 3.

Our result is currently the most sensitive exclusion limit on θ_{24} for Δm^2_{41} between about 0.1 eV^2 and 1 eV^2. It is worth mentioning that the region shown where sterile neutrinos are expected to be found is obtained by global fits [21,22] and depends on the assumed value of $|U_{e4}|^2$ which we cannot measure with this analysis. Even after the inclusion of our results to the global fits there are still regions where sterile neutrinos are not excluded and could explain the known anomalies [23,24].

4 Search for sterile neutrinos at low energy

The results in this section are published in Ref. [25].

As a starting point for any neutrino oscillation analysis in DeepCore it is essential to apply efficient rejection algorithms to reject atmospheric muon events reaching DeepCore. Most of this rejection is done using the remaining part of the IceCube detector as an active veto. This

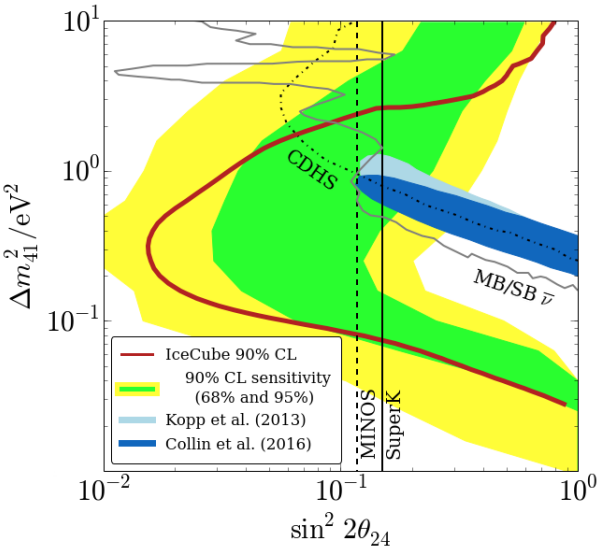

Figure 3 – Results from the IceCube high energy sterile search [16] for 90% CL (red line). For comparison the 90% CL expected sensitivity for our result is also shown for 68% (green) and 90% (yellow) of trials. In addition to that 90% CL exclusion limits from previous experiments [18,19,20] and the 99% CL allowed region from global fits to appearance data [21,22] with $|U_{e4}|^2 = 0.023$ or $|U_{e4}|^2 = 0.027$ are shown for comparison.

analysis uses the sample of neutrinos from our last published ν_μ disappearance result [26] using 3 years of data. This sample focus on "golden" ν_μ CC events, that is, events where a clear μ track is observed with many photons arriving with the Cherenkov light front (direct light), to ensure good reconstruction quality.

This search is also performed by fitting possible sterile neutrino signatures to the observed $E \times \cos\theta_z$ distribution, accounting for possible systematic errors coming from the uncertainties on the neutrino flux, neutrino cross section, standard neutrino oscillation parameter uncertainties, detector and fitting also for the remaining atmospheric muon background that might have remained in the sample after all cuts. We use data driven estimates for the remaining muon background shape as simulating enough atmospheric muons is very challenging.

No significant deviation from the null hypothesis was observed, and therefore we put the constraint on $|U_{\mu 4}|^2 \times |U_{\tau 4}|^2$ shown in Fig. 4. Our results provide the best constraints on $|U_{\tau 4}|^2$.

5 Precision measurement of atmospheric neutrino oscillations

The results in this section have not yet been published, however an article about these results is being prepared currently.

Since our previous published result [26], we have developed a new and improved event reconstruction that is able to reconstruct all events, instead of just those with a large amount of direct light. This was achieved by performing a likelihood-based reconstruction of all events taking into account the scattered light in the natural medium. We have also improved the event selection to allow us to perform a full-sky analysis, rather than looking exclusively for up-going neutrinos, which is beneficial as the down-going sample helps constrain systematic effects. With these changes the resulting 3 year sample has an order of magnitude more events.

Given all types of events can be reconstructed with this new reconstruction tool, it was essential to split the sample in two parts depending on which of the event topologies described in Sec. 2 we associate the event. The "track-like" sample is defined to contain mostly ν_μ CC events, while the "cascade-like" sample will contain the remaining events and is roughly equally divided between ν_μ CC events (that have a muon which is not observed) and events without a muon in the final state (typically ν_e CC and ν NC events).

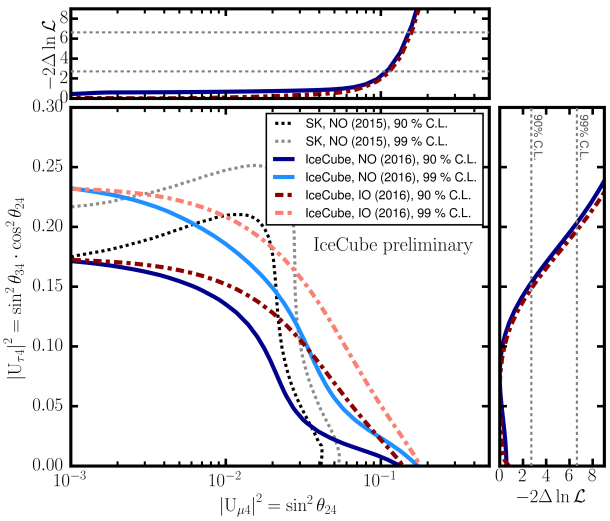

Figure 4 – Results from the IceCube low energy sterile search [25] assuming normal (solid lines) and inverted (dash-dotted lines) ordering. For comparison the results obtained by Super-Kamiokande [18] (dotted lines) are also shown. The outer plots show the result of 1-D projections after profiling over the other variables.

To measure the atmospheric mixing parameters, we fit jointly the $E \times \cos\theta_z$ distribution for both the track-like and cascade-like samples, accounting for a similar set of systematics used in Sec. 4. As for that analysis we use a data-driven background estimation. In this fitting we also include additional terms to the fitter to account for the statistical uncertainty in the prediction and a shape uncertainty from the data-driven background estimation.

The result obtained, using the approach of Feldman and Cousins [27] to ensure proper coverage, is shown in Fig. 5. Our results are consistent with those obtained by other experiments [28,29,30,31], even though we observed neutrino oscillations at a significantly higher energy and are thus subject to a very different set of systematic uncertainties.

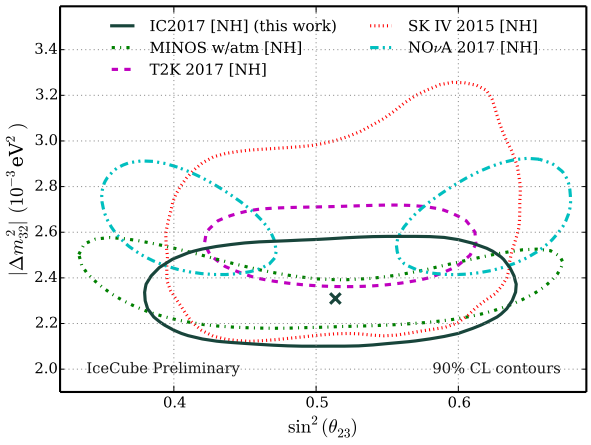

Figure 5 – The 90% CL allowed region for the measurement of the atmospheric neutrino mixing parameters with IceCube (solid line), with the cross indicating our best fit point. For comparison the results obtained by other experiments [28,29,30,31] are also shown (dashed lines).

6 Conclusions

Since being used for the discovery of neutrino oscillations, atmospheric neutrinos are still a valuable tool to study this phenomenon. Using atmospheric neutrinos, IceCube has produced world leading searches for sterile neutrinos [16,25] placing constraints in their phase space. We

have also continued using atmospheric neutrinos to improve the precision of our muon neutrino disappearance result producing very competitive results to those from leading experiments, and performing such measurement at a very different energy region, which permits additional testing of the neutrino oscillation framework. All studies presented here are still statistically limited, and refinements to these analyses are being prepared.

References

1. Y. Fukuda *et. al.*, (Super-Kamiokande) *Phys. Rev. Lett.* **81** 1562 (1998).
2. Q. R. Ahmad *et. al.*, (SNO) *Phys. Rev. Lett.* **89** 011301 (2002).
3. K. A. Olive *et. al.*, (Particle Data Group) *Chin. Phys.* **C38** 090001 (2014).
4. A. Aguilar-Arevalo *et. al.*, (LSND) *Phys. Rev.* **D64** 112007 (2001).
5. S. Schael *et. al.*, (SLD Electroweak Group, DELPHI, ALEPH, SLD, SLD Heavy Flavour Group, OPAL, LEP Electroweak Working Group, L3) *Phys. Rept.* **427** 257 (2006).
6. B. Armbruster *et. al.*, (KARMEN) *Phys. Rev.* **D65** 112001 (2002).
7. K. N. Abazajian *et. al.* "Light Sterile Neutrinos: A White Paper," [arXiv:1204.5379].
8. M. G. Aartsen *et. al.*, (IceCube) *JINST* **12** P03012 (2017), [arXiv:1612.05093].
9. M. G. Aartsen *et. al.*, (IceCube) *Phys. Rev. Lett.* **113** 101101 (2014), [arXiv:1405.5303].
10. R. Abbasi *et. al.*, (IceCube) *Astropart. Phys.* **35** 615 (2012), [arXiv:1109.6096].
11. S. T. Petcov *Phys. Lett.* **B434** 321 (1998), [arXiv:hep-ph/9805262].
12. M. Chizhov *et. al.* "On the oscillation length resonance in the transitions of solar and atmospheric neutrinos crossing the earth core," [arXiv:hep-ph/9810501].
13. E. K. Akhmedov *et. al. JHEP* **05** 077 (2007), [arXiv:hep-ph/0612285].
14. E. K. Akhmedov *et. al. JHEP* **06** 072 (2008), [arXiv:0804.1466].
15. A. M. Dziewonski and D. L. Anderson *Phys. Earth Planet. Interiors* **25** 297 (1981).
16. M. G. Aartsen *et. al.*, (IceCube) *Phys. Rev. Lett.* **117** 071801 (2016), [arXiv:1605.01990].
17. M. G. Aartsen *et. al.*, (IceCube) *Phys. Rev. Lett.* **115** 081102 (2015), [arXiv:1507.04005].
18. K. Abe *et. al.*, (Super-Kamiokande) *Phys. Rev.* **D91** 052019 (2015).
19. P. Adamson *et. al.*, (MINOS) *Phys. Rev. Lett.* **107** 011802 (2011).
20. G. Cheng *et. al.*, (SciBooNE, MiniBooNE) *Phys. Rev.* **D86** 052009 (2012).
21. J. Kopp *et. al. JHEP* **05** 050 (2013), [arXiv:1303.3011].
22. J. M. Conrad *et. al. Adv. High Energy Phys.* **2013** 163897 (2013), [arXiv:1207.4765].
23. S. Gariazzo *et. al.* "Updated Global 3+1 Analysis of Short-BaseLine Neutrino Oscillations," [arXiv:1703.00860].
24. G. H. Collin *et. al. Phys. Rev. Lett.* **117** 221801 (2016), [arXiv:1607.00011].
25. M. G. Aartsen *et. al.*, (IceCube) "Search for sterile neutrino mixing using three years of IceCube DeepCore data," [arXiv:1702.05160]. Submitted to *Phys. Rev.* D.
26. M. G. Aartsen *et. al.*, (IceCube) *Phys. Rev.* **D91** 072004 (2015), [arXiv:1410.7227].
27. G. J. Feldman and R. D. Cousins *Phys. Rev.* **D57** 3873 (1998).
28. K. Abe *et. al.*, (T2K) "First combined analysis of neutrino and antineutrino oscillations at T2K," [arXiv:1701.00432].
29. P. Adamson *et. al.*, (NOvA) "Measurement of the Neutrino Mixing angle θ_{23} in NOvA," [arXiv:1701.05891].
30. P. Adamson *et. al.*, (MINOS) *Phys. Rev. Lett.* **110** 251801 (2013).
31. R. Wendell *et. al.*, (Super-Kamiokande) *AIP Conf. Proc.* **1666** 100001 (2015).